NONLINEAR ANALYSIS OF REINFORCED CONCRETE SLABS WITH OPENINGS

Mohie ElDin S. Shukry
Structural Engineering Department, Faculty of Engineering,
Alexandria University, Alexandria, Egypt.

ABSTRACT

This paper presents a numerical study using the Finite Element Method for the analysis of reinforced concrete slabs with openings and subjected to distributed loads. The slab edges may be simply supported or have any boundary conditions, while the hole edges were considered free. The main parameters influencing the behavior of concrete in reinforced concrete members were taken into account in the analysis; such as concrete nonlinearity in compression and cracking in tension. The results reveal that the presence of openings caused a reduction in both the cracking load and the ultimate capacity of the slabs. The value of this reduction depended on the location of openings.

INTRODUCTION

Reinforced concrete slabs with openings may occur in practice such as location of ducts in residential buildings and hotels, and holes for lighting and ventilation in roofs of industrial buildings and water tanks.

Plate bending theory is not applicable for such cases where steep moment gradients may occur or where drastic variation in the cross section takes place. Numerical methods such as the Finite Element Method provide reasonable solutions for these cases if the shear deformations are considered in the analysis.

Korshay et al [1] analyzed rectangular elastic plates with centric rectangular holes using Finite Difference and the Successive Over Relaxation (SOR) method. Both the plate and the hole had different boundary conditions. Yield Line analysis was used [2, 3] to derive equations and charts for the ultimate strength of the two way reinforced concrete slabs with central openings.

FINITE ELEMENT ANALYSIS

A nonlinear FE analysis was used in the present study. The element used is a specialization of the hexahedral solid element developed by Ahmad et al [4] and is applied for the analysis of both thick and thin plates [5]. The element consists of eight nodes (corners and mid-sides) with three degrees of freedom at each node; a vertical translation w, a rotation about x-axis θ_x, and a rotation about y-axis θ_y. In the derivation of the element stiffness matrix, the constraint of straight normals was introduced , as assumed in the classical plate bending theory [6], but deformed edges need not remain normal. Therefore, the transverse shear effects were included. The advantage with this element is that the plate can experience bending and transverse shear deformations.

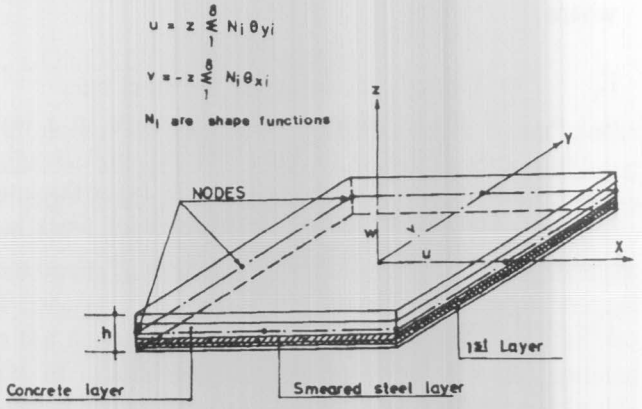

Figure 1. Layered plate element.

The element was divided across its thickness into a number of layers (Figure (1)) with the steel reinforcement smeared into a concrete layer. Perfect bond was assumed between the layers and between

concrete and steel. Five values of non-zero stresses (σ_x, σ_y, τ_{xy}, τ_{yz}, τ_{zx}) and strains (ϵ_x, ϵ_y, γ_{xy}, γ_{yz}, γ_{zx}) were considered. The strain energy corresponding to stresses perpendicular to the middle surface was ignored (i.e. $\sigma_z = 0$). One mesh 2 x 2 x 2 of gaussian integration points was used to derive the stiffness matrix of the layered element. Incremental/iterative procedure was chosen for the analysis using the Initial Stress formulations.

MATERIAL PROPERTIES

1. Steel Reinforcement

The reinforcing steel is assumed to be elastic-plastic with stiffness only in the bar direction. The stress-strain relationship for the steel is shown in Figure (2). The contribution of steel to the constitutive matrix of the concrete layer containing the steel can be expressed as:

$$[D_s] = \begin{bmatrix} \rho_x E_s & 0 & 0 & 0 & 0 \\ & \rho_y E_s & 0 & 0 & 0 \\ & & 0 & 0 & 0 \\ & & & 0 & 0 \\ \textit{symm.} & & & & 0 \end{bmatrix} \quad (1)$$

where

E_s = Young's modulus for the steel bars

ρ_x , ρ_y = the reinforcement percentage in a layer; i.e. the area of the steel per unit length in each direction divided by the layer thickness. The slabs studied in the present work were isotopically reinforced, i.e. $\rho_x = \rho_y$.

The steel stresses are given as:

$$\sigma_x = E_s \, \epsilon_x , \qquad \sigma_y = E_s \, \epsilon_y \quad (2)$$

When yielding of steel occurs, E_s in Eq. 2 is replaced by E_p; the plastic modulus of steel.

2. *Concrete in Compression*

The concrete in compression is treated as an isotropic linearly elastic-plastic strain-hardening material. The model used in the analysis is a simplification of the rate-independent elastic-plastic theory of Chen and Chen [7]. The initial discontinuous (yield) surface and failure (crushing) surface are expressed in terms of the first stress invariant I_1 and the second invariant of deviatoric stress J_2.

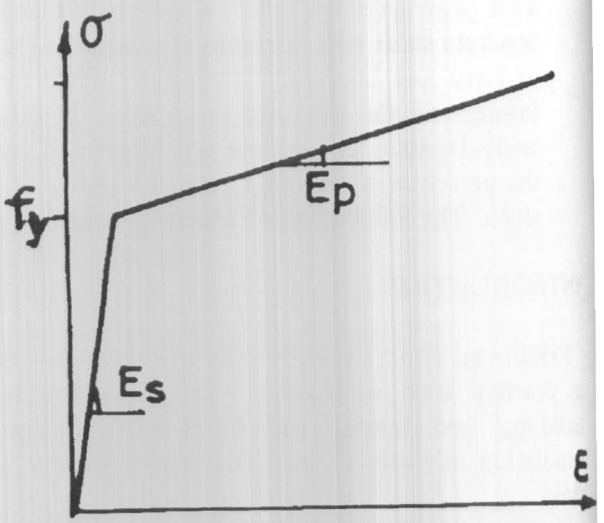

Figure 2. Idealized stress-strain relationship for steel bars.

Initially, concrete is assumed as an isotropic linear elastic material and its stress-strain relationship is given by:

$$\{\Delta\sigma\} = [\, D_e \,] \{\Delta\epsilon\} \quad (3)$$

where

$$[D_e] = \frac{E_c}{1-\nu_c^2} \begin{bmatrix} 1 & \nu_c & 0 & 0 & 0 \\ & 1 & 0 & 0 & 0 \\ & & \frac{1-\nu_c}{2} & 0 & 0 \\ & & & \frac{1-\nu_c}{2*1.2} & 0 \\ \textit{symm.} & & & & \frac{1-\nu_c}{2*1.2} \end{bmatrix} \quad (4)$$

E_c = Young's modulus for concrete,

ν_c = Poisson's ratio for concrete

The factor 1.2 appears in the last two rows of Eq. 4 because transverse stresses vary parabolically through the thickness and the shear load is found from the mean stress but the strain energy is found from the mean squared stress.

The yield surface is the limiting surface for the elastic concrete behavior. In the present study, this surface is given by [8] :

$$0.1775\ I_1 + \sqrt{0.0315\ I_1^2 + 4.065\ J_2} - \sigma_0 = 0 \quad (5)$$

where σ_o = effective (equivalent) stress and is taken as 0.3 f_c for the initial yield surface,

f_c = concrete compressive strength

Beyond the elastic limit (Eq. 5), the normality condition (associated plastic flow) is assumed to govern the post-yielded stress-strain relations of concrete, i.e.

$$\{\Delta\sigma\} = [D_{ep}]\ \{\Delta\epsilon\} \quad (6)$$

where D_{ep} = elastic-plastic material matrix

$$[D_{ep}] = D_e - \frac{D_e \left\{\frac{\partial\sigma_0}{\partial\sigma_{ij}}\right\} \left\{\frac{\partial\sigma_0}{\partial\sigma_{ij}}\right\}^T D_e}{H + \left\{\frac{\partial\sigma_0}{\partial\sigma_{ij}}\right\}^T D_e \left\{\frac{\partial\sigma_0}{\partial\sigma ij}\right\}} \quad (7)$$

σ_{ij} = stress tensor

$\{\partial\sigma_o/\partial\sigma_{ij}\}$ = a vector normal to the current loading surface which is expressed as:

$$\sigma_0 = 0.1775\ 1_1 + \sqrt{0.0355 I_1^2 + 4.065\ J_2},\ 0.3 f_c \le \sigma_0 \le f_c \quad (8)$$

H = hardening parameter

The value of H may be obtained from the extrapolation of results from uniaxial relationship between stresses and plastic strain ϵ_p. According to Reference 8,

$$H = E_c\ [\sqrt{\epsilon_0 / 2\ \epsilon_p} - 1] \quad (9)$$

where ϵ_o = total strain at peak stress f_c in uniaxial test = 2 f_c / E_c,

$$e_p^2 - 2\sqrt{2\epsilon_0} e_p^{3/2} + 2\epsilon_0 e_p - \sigma_0^2 / E_c^2 = 0 \quad (10)$$

which is solved by iteration procedure for ϵ_p .

The yield surface, in stress space, extends isotopically as plastic strains occur up to a limiting value, which defines failure. In the present work, the failure surface is expressed by Eq. 5 with σ_o = f_c. Figure (3) shows both the yield surface and the failure surface on biaxial principal stress axes. Softening of concrete in compression after reaching the failure surface is neglected in the present analysis.

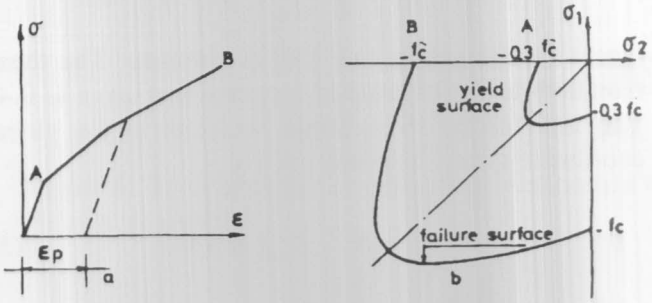

Figure 3. Concrete modeling in compression
a. stress versus total strain
b. yield and failure surfaces on biaxial principal stress plane.

3. CONCRETE IN TENSION

Concrete in tension is modelled as a linear elastic material without strain softening or tension stiffening effects. Smeared cracking approach was adopted in the present work. A crack is assumed to occur when the maximum principal stress exceeds the tensile strength of concrete. The crack will form in a plane orthogonal to the maximum principal stress. A maximum of two sets of cracks are allowed to form at each gaussian point. Orthogonal fixed crack model is adopted in this study, i.e. the direction of the first set of cracks is fixed during the entire computional process and the maximum stress in the plane parallel to the existing crack is calculated and if this stress exceeds the tensile strength of concrete then a new set of cracks is formed perpendicular to it. If n,s and t are axes of orthotropy, where n refers to the direction normal to the crack,

crack is calculated and if this stress exceeds the tensile strength of concrete then a new set of cracks is formed perpendicular to it. If n,s and t are axes of orthotropy, where n refers to the direction normal to the crack, then the orthotopic constitutive matrix for the cracked concrete in the crack plane is expressed as:

$$\{\Delta\sigma\}^* = [D_{cr}] \{\Delta\epsilon\}^*$$

i.e.

$$\begin{Bmatrix} \Delta\sigma_n \\ \Delta\sigma_{nt} \\ \Delta\sigma_{ns} \end{Bmatrix} = \begin{bmatrix} 0 & 0 & 0 \\ 0 & 0.4G & 0 \\ 0 & 0 & 0.4G \end{bmatrix} \begin{Bmatrix} \Delta\epsilon_n \\ \Delta\gamma_{nt} \\ \Delta\gamma_{ns} \end{Bmatrix} \quad (12)$$

where G is the shear modulus of concrete. The shear retention factor for cracked concrete was taken as 0.4. The incremental stress-strain relations in the global coordinate system is given by:

$$\{\Delta\sigma\} = N^T [D_{cr}] N \{\Delta\epsilon\} \quad (13)$$

where [N] is a 3 x 5 transformation matrix reflecting the orientation of the crack and is given by:

$$[N] = \begin{bmatrix} l_1^2 & m_1^2 & l_1m_1 & m_1n_1 & n_1l_1 \\ 2l_1l_2 & 2m_1m_2 & l_1m_2+l_2m_1 & m_1n_2+m_2n_1 & n_1l_2+n_2l_1 \\ 2l_3l_1 & 2m_3m_1 & l_3m_1+l_1m_3 & m_3n_1+m_1n_3 & n_3l_1+n_1l_3 \end{bmatrix} \quad (14)$$

where l_1, m_1 and n_1 form a vector which dictates the direction of the local n-axis expressed in the global direction.

The effect of tensile strains normal to the crack on the compressive strength of concrete in a direction parallel to crack is neglected.

A computer nonlinear finite element program is developed to implement the above material parameters and it was run on VAX 3500 computer at Faculty of Engineering, Alexandria University.

NUMERICAL EXAMPLES

To investigate the validity of the present analysis, the following problems were solved:

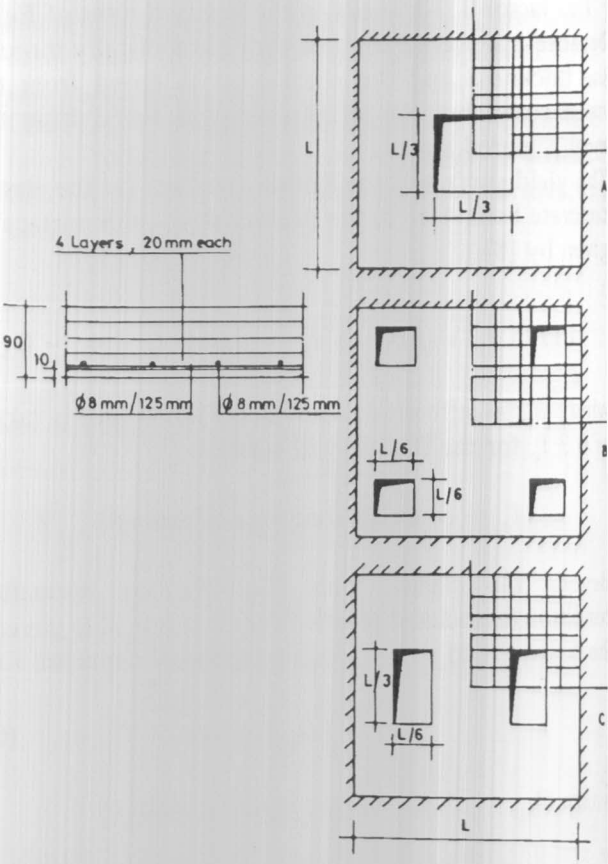

Figure 4. Dimensions, reinforcement and properties o slabs.

a- Square plate with holes; elastic analysis

Three cases of hole positions, as shown in Figure (4) were studied and the results are given in Table 1. Fo all the three cases, the total area of the holes was kep constant and it was about 0.11 the total area of th plate. Table 1 indicates that the highest values o deflection and moments were obtained for case B where four holes were moved diagonally towards th corners, followed by case C ,where two holes wer moved in one direction. For all the three cases, bot deflection and moments were higher than those for th solid plate without holes. The maximum deflection fo cases B and C occurred at the plate center while th maximum moments for the three cases occurred at th hole corners. Figure (5) shows the distribution of th bending moment at different sections for all the cases As shown in the figure, severe disturbances o moments occurred at the hole edges and thi disturbance extended for a large distance away fro

the holes. Also, small values of negative bending moments occurred around the hole boundaries.

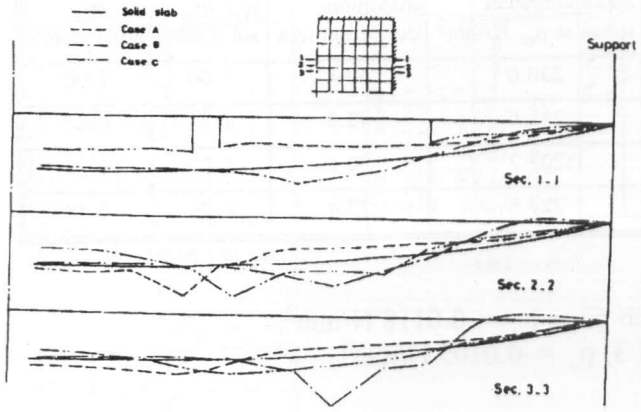

Figure 5. Distribution of bending moments at different sections.

Table 1. Results of the elastic analysis.

Cause Studied	Maximum Deflection[1]		Maximum Moment[2]	
	analysis	exact	analysis	exact
solid plate	0.00407	0.00406[3]	0.044	0.0423[3]
case A	0.00416	-------	0.056	------
case B	0.00456	-------	0.063	------
case C	0.00440	-------	0.058	------

(1) w = coeff. * p L^4 /D
(2) moment = coeff. * p L^2
(3) Reference 6

b- Simply supported slab under uniform load; nonlinear analysis

Figure (6-a) shows the dimensions and reinforcement of a slab supported on all four edges which was studied experimentally by Taylor et al [9]. The center point deflection is plotted against the total load applied to the slab in Figure (6-b) together with the results obtained from the Finite Element analysis.
As shown in Figure (6), the FE analysis predicted well the slab behavior but the predicted ultimate load was less than that obtained experimentally. It should be noted that excessive deflections were recorded experimentally without slab failure and the additional strength may be due to the effects of the membrane a action.

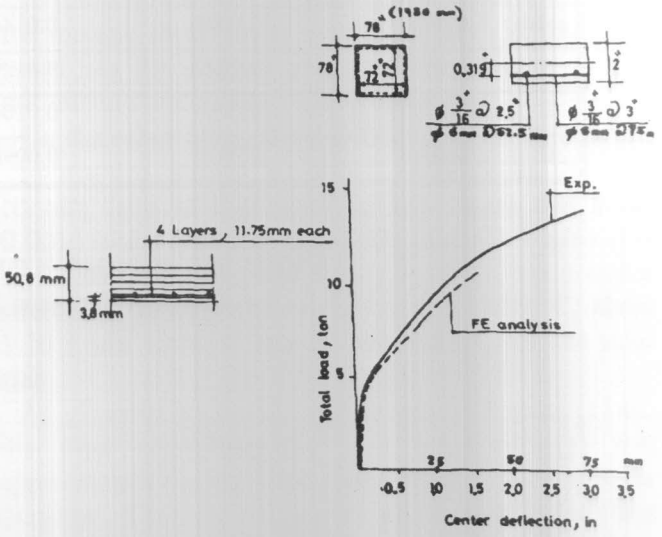

Figure 6. Total load-center deflection relationship for taylor et al slab [9].

c- Simply supported RC slab with different hole positions under uniform load

Four reinforced concrete slabs were analyzed up to failure; a solid slab and three slabs with openings at different positions (slabs A, B and C). Details of slab dimensions, reinforcement and materials strength are given in Figure (4). The main results of the analyses are given in Table (2). The table indicates that the presence of openings in slabs greatly affected both the cracking load and the ultimate capacity. Analysis of slab with holes placed diagonally (slab B) produced 43% reduction in the cracking load compared to that for solid slab while for the slab with holes placed eccentric along one direction (slab C) a 32% reduction in the ultimate capacity was obtained. However, only 17% reduction in the ultimate capacity was obtained for the slab with centric hole (slab A).
Figure (7) displays the load-deflection relationship for all the slabs. All slabs showed the same initial stiffness up to the cracking load when a remarkable reduction in stiffness occurred for the slabs with openings and this reduction continued up to failure.

Table 2.

slab	cracking load; p_{cr}, N/mm^2	load at initial concrete yield, N/mm^2	ultimate load; p_u* N/mm^2	maximum steel stress at p_u, N/mm^2	maximum deflection mm	p_{cr}/ (p_{cr} solid slab)	p_u/ (p_u solid slab)
solid	0.0065	0.0088	0.0144	230.0	59.4	1.00	1.00
A	0.0047	0.0072	0.0120	234.6	42.3	0.72	0.83
B	0.0037	0.0064	0.0104	207.7	30.8	0.57	0.72
C	0.0048	0.0070	0.0098	227.8	27.4	0.74	0.68

* Yield line analysis for solid slab gives $p_u = 0.0118$ N/mm^2, for slab A (references 2 and 3) $p_u = 0.0105$ N/mm^2.

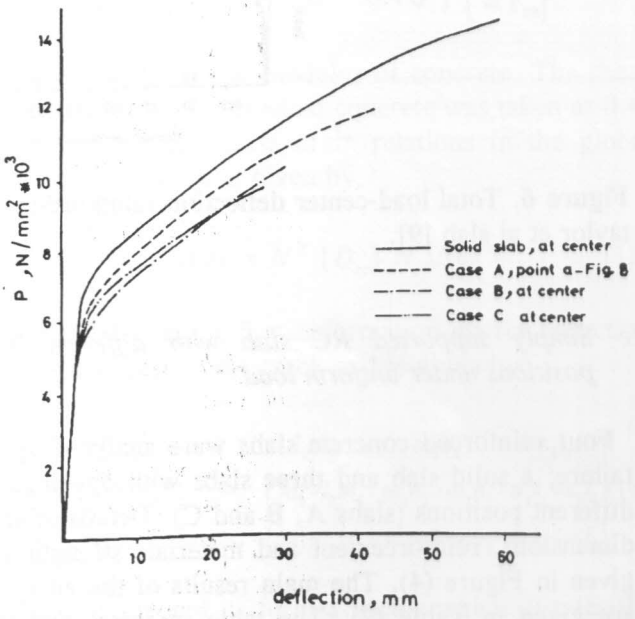

Figure 7. Load-deflection relationship for slabs.

Figures (8), (9) and (10) show the cracking patterns for the slabs with openings. At loads ranged from 36% to 49% of the ultimate capacity, cracks on the bottom surface started around the hole corners and then spread away with load increase and penetrated the slab thickness to reach the mid-depth at loads ranged from 67% (slab A) to 86% (slab C) of the ultimate capacity. Cracks on the top surface of the slabs occurred in the three cases and their number was remarkable in slab B, as shown in Figure (10.c) A drop in stiffness was obtained for slab C after the cracks reached mid-depth of the slab in most elements.

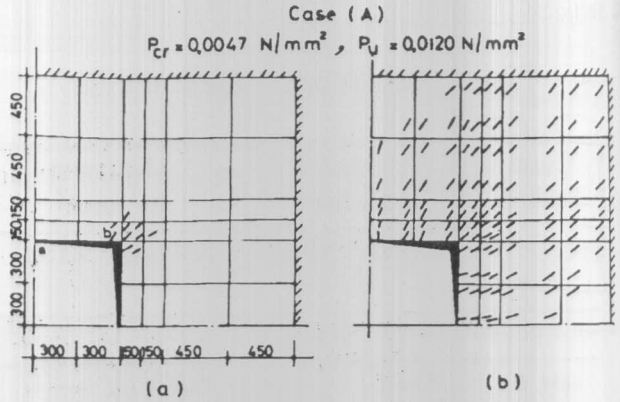

Figure 8. Cracking patterns on the bottom surface of slab A a. at p = 0.0048 N/mm^2 = 40 % of p_u
b. at p = 0.0096 N/mm^2 = 80 % of p_u.

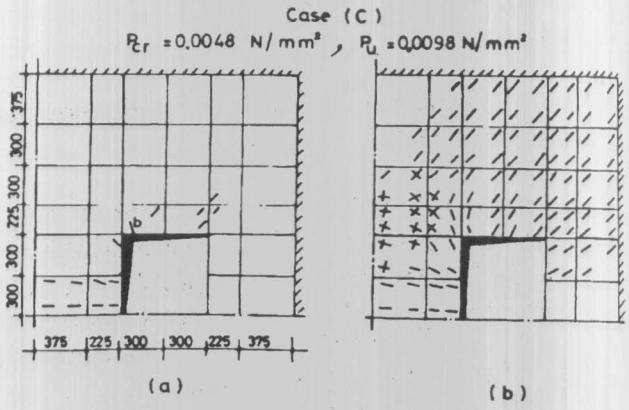

Figure 9. Cracking patterns on the bottom surface of slab C a. at p = 0.0056 N/mm^2 = 57 % of p_u
b. at p = 0.0084 N/mm^2 = 86 % of p_u.

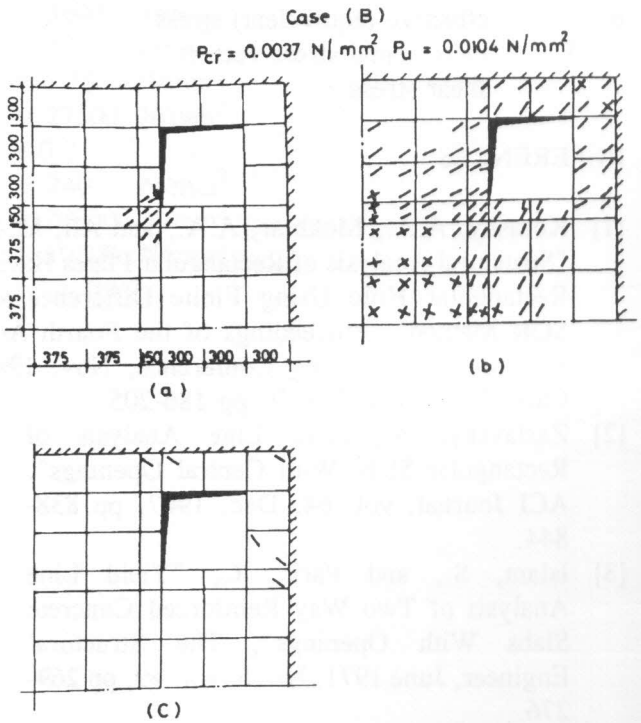

Figure 10. Cracking patterns for slab B
a. bottom surface at p = 0.0048 N/mm^2 = 46 % of p_u
b. bottom surface at p = 0.0088 N/mm^2 = 85 % of p_u
c. top surface at p_u.

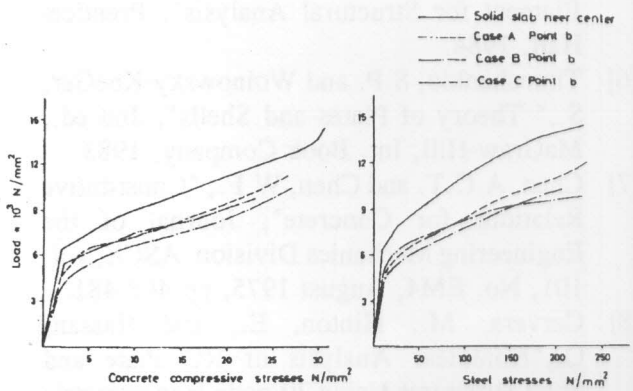

Figure 11. Load-increase in concrete and steel stresses
a. increase in concrete compressive stresses
b. increase in steel tensile stresses.

Figure (11) shows the change in concrete and steel stresses with load increase. Initial yield of concrete in compression, defined by Eq. 5, occurred first at the elements located near corners of holes and also at the slabs corner. The load level at which this yield occurred was about 60 % of p_u for slabs A and B and 70 % of p_u for slab C. The occurrence of concrete yield , at early stages of loading, at the slab corners was due to high values of inplane shear stresses existed at these corners. For example, the value of the inplane shear strain at failure of slab A was about 0.0023 and the inplane shear stress was 13 N/mm^2. It should be noted that the element used in the present work does not include inplane degrees of freedom.

On the other hand, the maximum values of concrete compressive strains recorded away from the slab corners (and at mid-depth of top layer) was about 0.0016 (slabs A and B) and 0.001 (slab C). Figure (11-a) indicates that the maximum concrete compressive stresses at failure were equal to f_c for slab C, about 1.10 f_c for slabs A and B, and 1.23 f_c for the solid slab.

As given in Table (2) and shown in Figure (11-b), the steel reinforcement (near hole corners) was approximately at its yield stress when failure of slabs occurred. The percentage of reinforcement in the slabs was 0.57 %. Figure (11-b) also indicates that a sudden increase in steel stress occurred in slab C at about 70 % of p_u.

CONCLUSIONS

In this paper, a nonlinear finite element analysis was developed to predict the behavior of reinforced concrete slabs with openings and subjected to uniformly distributed load. Conclusions derived from this work include the following :

1- The presence of openings in slabs caused a reduction in the ultimate capacity compared to that of solid slabs without openings having the same dimensions, materials and reinforcement. This reduction depends on the opening size and position. For the slabs studied in the present work it ranged from 17% to 32%. The reduction in the cracking loads was generally higher and ranged 26% - 43%.
2- A concentration of stresses occurred at the hole corners where cracks at the tension side of the slabs initiated and maximum stresses in concrete and steel were recorded.
3- Cracks at the top surface of the slabs occurred around the hole boundaries.
4- Due to the type of the element used in the

present work, high values of inplane shear stresses were obtained at the slab corners. However, there was no indication that these stresses affected the overall behavior of the slabs.

NOTATION

D	flexural rigidity of the slab
$[D_{cr}]$	stress-strain matrix for cracked concrete in the crack plane
$[D_e]$	elastic stress-strain matrix
$[D_{ep}]$	elastic-plastic material matrix
$[D_s]$	stress-strain matrix for reinforcement smeared into concrete layer
E_c	Young's modulus of concrete
E_s	Young's modulus of steel
E_p	plastic modulus of concrete
f_c	concrete compressive strength
f_t	concrete tensile strength
f_y	yield stress of steel
G	shear modulus of concrete
H	hardening parameter
h	slab thickness
I_1	first stress invariant
J_2	second invariant of deviatoric stress
L	span of square slab
l,m and n	direction cosines of principal stress to x,y and z axes respectively
[N]	transformation matrix
p	intensity of uniformly distributed load
p_{cr}	cracking load
p_u	ultimate (failure) load
u,v	displacements along x and y axis respectively
w	deflection of the slab
ϵ	normal strain
ϵ_o	total strain at peak stress f_c in uniaxial test
ϵ_p	equivalent plastic strain
$\{\Delta\epsilon\}$	incremental strain vector
γ	shear strain
ν_c	Poisson's ratio for concrete
ρ_x, ρ_y	reinforcement ratio in a layer in x and y direction respectively
σ	normal stress
σ_{ij}	stress tensor
σ_o	effective (equivalent) stress
$\{\Delta\sigma\}$	incremental stress vector
τ	shear stress

REFERENCES

[1] Korashy, A.A., Mokhtar, A.A., and Ali, M.A., "Structural Analysis of Rectangular Plates Having Rectangular Hole Using Finite Difference and SOR Method", Proceedings of the Fourth Arab Structural Engineering Conference, Nov. 1991, Cairo University, Part II, pp 186-205.

[2] Zaslavsky, A.,"Yield Line Analysis of Rectangular Slabs With Central Openings", ACI Journal, vol. 64, Dec. 1967, pp 838-844.

[3] Islam, S., and Park, R., "Yield Line Analysis of Two Way Reinforced Concrete Slabs With Openings", The Structural Engineer, June 1971, No. 6, vol. 49, pp 269-276.

[4] Ahmad, S., Irons, B.M., and Zienkiewicz, O.C., "Analysis of Thick and Thin Shells by Curved Finite Element", Int. Jo. Num. Meth. Eng., vol. 3, No. 4, 1971, pp 575-586.

[5] Weaver, W. and Johnston, P.R., "Finite Element for Structural Analysis", Prentice-Hall, 1984.

[6] Timoshenkio, S.P. and Woinowsky-KneGer, S.," Theory of Plates and Shells", 2nd ed., MaGraw-Hill, Int. Book Company, 1983.

[7] Chen, A.C.T. and Chen, W.F., "Constitutive Relations for Concrete", Journal of the Engineering Mechanics Division, ASCE, vol. 101, No. EM4, August 1975, pp 465-481.

[8] Cervera, M., Hinton, E., and Hassan, O.,"Nonlinear Analysis of RC Plate and Shell Structures Using 20-node Isoparametric Brick Element", Computers and Structures, vol. 25, No. 6, pp 845-869, 1987.

[9] Taylor, R., Maher, D.R.H., and Hayes, R.," Effect of the Arrangement of Reinforcement on the Behavior of Reinforced Concrete Slabs", Magazine of Concrete Research, vol.98, No.55, June 1966.

$L = 3600$ mm
$f_c = 25$ N/mm^2
$f_t = 2.75$ N/mm^2
$E_c = 27500$ N/mm^2
$\nu_c = 0.2$
$f_y = 240$ N/mm^2
$E_s = 200000$ N/mm^2
$E_p = 10200$ N/mm^2
$\rho_x, \rho_y = 0.02$

$L = 1828.8$ mm
$f_c = 36$ N/mm^2
$f_t = 3.6$ N/mm^2
$E_c = 30000$ N/mm^2
$\nu_c = 0.2$
$f_y = 375$ N/mm^2
$E_s = 206000$ N/mm^2
$E_p = 10000$ N/mm^2
$\rho_x, \rho_y = 0.0238$